Robotica (2006) volume 24, pp. 401–410. © 2006 Cambridge University Press
doi:10.1017/S0263574705002316 Printed in the United Kingdom

Controlling a bipedal walking robot actuated by pleated pneumatic artificial muscles

Bram Vanderborght*, Björn Verrelst, Ronald Van Ham & Dirk Lefeber

Vrije Universiteit Brussel, Department of Mechanical Engineering, Pleinlaan 2, 1050 Brussels (Belgium)

(Received in Final Form: August 26, 2005. First published online: March 2, 2006)

SUMMARY

This paper reports on the control structure of the pneumatic biped Lucy. The robot is actuated with pleated pneumatic artificial muscles, which have interesting characteristics that can be exploited for legged locomotion. They have a high power to weight ratio, an adaptable compliance and they can absorb impact effects.

The discussion of the control architecture focuses on the joint trajectory generator and the joint trajectory tracking controller. The trajectory generator calculates trajectories represented by polynomials based on objective locomotion parameters, which are average forward speed, step length, step height and intermediate foot lift. The joint trajectory tracking controller is divided in three parts: a computed torque module, a delta-p unit and a bang-bang pressure controller. The control design is formulated for the single support and double support phase, where specifically the trajectory generator and the computed torque differs for these two phases.

The first results of the incorporation of this control architecture in the real biped Lucy are given. Several essential graphs, such as pressure courses, are discussed and the effectiveness of the proposed algorithm is shown by the small deviations between desired and actual attained objective locomotion parameters.

KEYWORDS: Bipedal walking robot; Pleated pneumatic artificial muscle; Dynamic control.

I. INTRODUCTION

Most of the bipeds today use electrical actuation. Motor drives and their control are well known but have some important limitations. Since for robotic applications the rotational speed of the limb joints is much lower than the nominal speed of most electrical motors, transmission units are almost always required. These increase the weight and complexity of the actuation system and induce high reflected inertia. The latter is awkward for shock absorbance, especially when robots are expected to walk faster. For manipulator robot implementation, stiff joints have always been favorable above compliant joints since they increase tracking precision. For legged robots however, tracking precision is not that stringent as overall dynamic stability. Compliant joint properties can then be exploited to store motion energy, reduce control effort and absorb impact shocks.

One of the first to incorporate compliant joint properties for legged locomotion was Matsuoko,[1] and later Raibert[2] by means of a pneumatic cilinder. Later Pratt developed the "Series Elastic Actuators"[3] with inherent compliance, used for the two legged "Spring Flamingo"[4] and consist of a motor drive with a spring in series. The disadvantage of such a setup is that the stiffness can't be changed. Takanishi developed the two-legged walker WL-14,[5] where a complex non-linear spring mechanism makes predefined changes in stiffness possible. The Robotics Institute at Carnegie Mellon University developed the "Actuator with Mechanically Adjustable Series Compliance" (AMASC).[6] This actuator is designed for use in a highly dynamic legged robot. It has fiberglass springs with a large energy storage capacity. A more elegant way to implement variable compliance is to use pneumatic artificial muscles, for which the applied pressures in the muscles determine both position and stiffness.[7] Research on pneumatic artificial muscles topic was done by Van der Linde,[8] Wisse,[9] Caldwell[10] and the Shadow Robot Company[11] by implementation of Mc Kibben muscles.

Our research focusses on the Pleated Pneumatic Artificial Muscle (PPAM); this actuator gives an alternative to the McKibben type muscle by trying to overcome some of the latter's shortcomings such as a high threshold of pressure and dry friction. Artificial muscles have a high power to weight ratio and can be directly coupled without complex gearing mechanisms. The elastic joint properties can be exploited to store motion energy, reduce control effort and absorb impact shocks. These properties can also be found in human skeleton muscles: it is well understood that leg compliance plays a crucial role in walking and running.

In spite of these benefits, pneumatic actuation has not been widely used as actuation system for legged locomotion, mainly because of it's extra design and control effort. In this context the biped Lucy has been constructed to study the feasibility of pneumatic muscles for bipedal locomotion and how adaptable joint compliance can be beneficial. In the publication of Verrelst[12] the control of these pneumatic artificial muscles was discussed for a one dimensional setup. This paper focusses on the control of the complete biped.

* Corresponding author. E-mail: bram.vanderborght@vub.ac.be. http://lucy.vub.ac.be

II. HARDWARE OF THE BIPED LUCY

II.1. Pleated pneumatic artificial muscle

A pneumatic artificial muscle is essentially a membrane that expands radially and contracts axially when inflated, while generating high pulling forces along the longitudinal axis. Different designs have been developed. The best known is the so called McKibben muscle.[13] This muscle contains a rubber tube which expands when inflated, while a surrounding netting transfers tension. Hysteresis, due to dry friction between the netting and the rubber tube, makes control of such a device rather complicated. Typical of this type of muscle is a threshold level of pressure before any action can take place. The main characteristic of the muscle designed at the Vrije Universiteit Brussel,[7,14] was to avoid friction, thus making control easier while avoiding the threshold. This was achieved by arranging the membrane into radially laid out folds that can unfurl free of radial stress when inflated. Tension is transferred by stiff longitudinal fibres that are positioned at the bottom of each crease. A photograph of the inflated state of the Pleated Pneumatic Artificial Muscle (PPAM) is given in figure 2. If we omit the influence of elasticity of the high tensile strength material used for the fibres, the characteristic for the generated force is given by:

$$F = pl^2 f\left(\epsilon, \frac{l}{R}\right) \tag{1}$$

where p is the applied gauge pressure, l the muscle's full length, R its unloaded radius and ϵ the contraction.

The dimensionless function f depends only on contraction and geometry, expressed by the broadness R/l. At low contraction, forces are extremely high causing excessive material loading, and the generated forces drop too low for large contraction. Thus contraction will be bounded between two limits, 5 and 35%, in practise. The graph in figure 1 gives the generated force for different pressures of a muscle with initial length 10 cm and unloaded diameter 2.5 cm. Forces up to 3000 N can be generated with gauge pressure of only 300 kPa while the device weighs about 100 g.

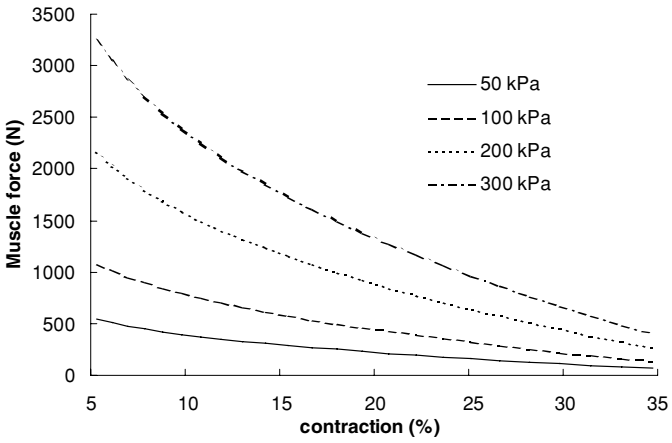

Fig. 1. Generated forces (N).

Fig. 2. Photograph of inflated state of the PPAM.

II.2. Antagonistic set-up

Pneumatic artificial muscles can only pull. In order to have a bidirectionally working revolute joint one has to couple two muscles antagonistically. A rod transmission was chosen because of its inherent asymmetrical operation about its central position, which can compensate the non-linear muscle characteristic. Depending whether the joint is a knee, ankle or hip the dimensions of the connection can be chosen in order to meet the needs of the specified joint function, not only in torque levels but also in range of motion.

Taking into account equation (1) and if r_1 and r_2 define the leverage arm of the extensor and flexor muscle respectively, the joint torque τ is given by following expression:

$$\begin{aligned}\tau = \tau_1 - \tau_2 &= p_1 l_1^2 r_1 f_1 - p_2 l_2^2 r_2 f_2 \\ &= p_1 t_1(\beta) - p_2 t_2(\beta)\end{aligned} \tag{2}$$

with p_1 and p_2 the applied gauge pressures in extensor and flexor muscle respectively which have lengths l_1 and l_2. The dimensionless force functions of both muscles are given by f_1 and f_2. The functions t_1 and t_2, in equation (2), are determined

https://doi.org/10.1017/S0263574705002316 Published online by Cambridge University Press

by the choices made during the design phase and depend on the joint angle β. Thus joint position is influenced by weighted differences in gauge pressures of both muscles. Moreover, it is shown (cfr [12]) that the compliance of a joint is dependant on the weighted sum of the pressures in both muscles. Thus torque, and consequently position, and compliance can be controlled separately.

II.3. The robot

The Multibody Mechanics Research Group of the Vrije Universiteit Brussel has built the planar walking biped "Lucy". The goal of the project is to achieve a lightweight bipedal robot which is able to walk in a dynamically stable way, while exploiting the passive behaviour of the PPAM's in order to reduce energy consumption and control efforts. In primary instance the compressor or supply tank and PC are placed outside the robot. Building an autonomous robot is not the major concern, the main focus of the research is to investigate if pneumatic muscles and compliant actuation in general are suitable for bipedal walking. The muscles are, however, strong enough to carry an additional payload. Figure 3 shows the robot Lucy which weighs less than 30 kg and is 150 cm tall. The motion of Lucy is restricted to the sagittal plane in order to avoid extra unnecessary complexity regarding control and design. Moreover, it has been shown[15] that for biped walking the dynamical effects in the lateral plane have a marginal influence on the dynamics in the sagittal plane.

Key elements in the design phase are modularity and flexibility regarding the ability to make changes to the robot configuration during the experimental process. This resulted in nearly the same configuration for each structural element such as lower-leg, upper-leg and body. The modularity is also incorporated in the control hardware. Every joint has its own 16-bit micro-controller (MC68HC916Y3 made by Motorola) which incorporates the bang-bang controller and collects sensor information. The used sensors are the HEDM6540 incremental encoder for reading the joint position and velocity and two pressure sensors inside each muscle of the antagonistic setup. The encoder and pressure signals are registered with a separate processor, TPU, on the micro-controller in order not to load the CPU whilst reading their values. An additional micro-controller is used to detect ground contact, absolute position of the body and compressed air consumption.

The high-level control is implemented on a PC. All the micro-controller units communicate with this central, Windows operated PC by a USB 2.0 high speed serial bus. As such, the complete biped is controlled at a sample rate of 2000 Hz. The timing of the communication refresh rate is controlled by the EZ-usb FX2 Cypress micro-controller. The local micro-controllers ensure low-level, quasi real-time, control of the joints, and in order to prevent control disturbance of missed torque calculations by the central PC, the incoming data of the local units are buffered in the dual ported RAM hardware. So whenever the central PC does not succeed to perform the necessary calculations within the sampling time, the local control units use the previously sent data, which are stored in the dual ported RAM. One should also remark in the context of this refresh rate, that the delay time of the valves is about 1 ms, which suggests that the communication frequency of 2000 Hz is high enough. More information on the hardware of Lucy can be found in reference [16].

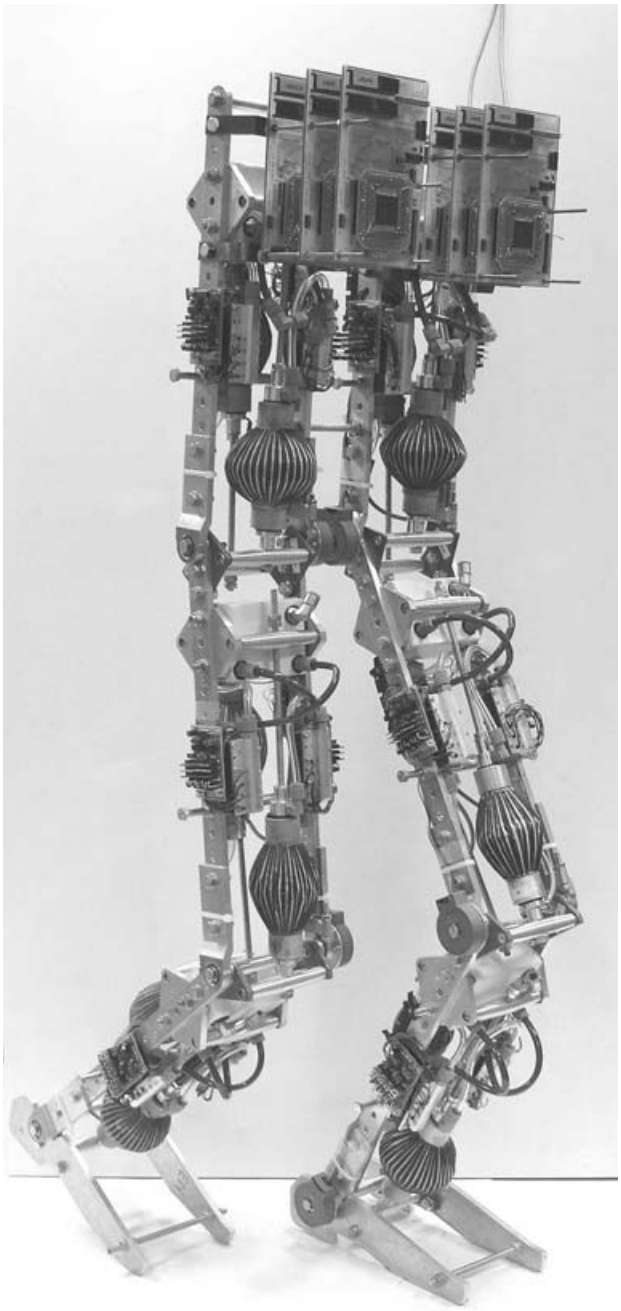

Fig. 3. Photograph of Lucy.

III. CONTROL ARCHITECTURE

The considered controller is given in the schematic overview of figure 4 and is a combination of a global trajectory generator and a joint trajectory tracking controller. The trajectory generator calculates polynomial joint trajectories out of the objective locomotion parameters chosen for a specific robot step. The tracking controller is divided into a computed torque controller, a delta-p unit and

https://doi.org/10.1017/S0263574705002316 Published online by Cambridge University Press

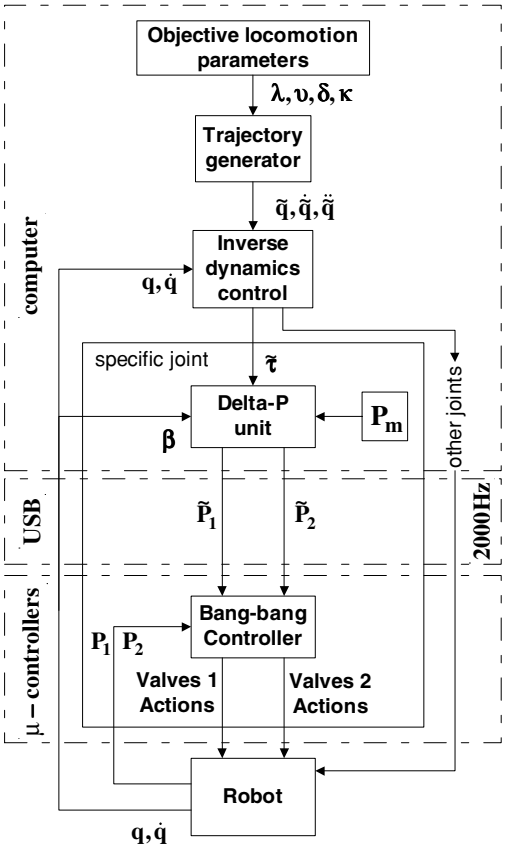

Fig. 4. Overview of the joint control architecture.

a pressure bang-bang controller. The computed torque controller calculates the required joint torques based on the robot dynamics. For each joint a delta-p unit translates the calculated torques into desired pressure levels for the two muscles of the antagonistic set-up. Finally the bang-bang controller determines the necessary valve actions to set the correct pressures in the muscles. The trajectory generator, computed torque and delta-p units are implemented on a central PC since these controllers require a substantial computational effort. The bang-bang controller is locally implemented on micro-controller units. In the next sections the different elements of the control structure are discussed in more detail.

III.1. Trajectory generator

The trajectory generation is designed to generate walking movements based on objective locomotion parameters chosen for a specific robot step, which are average forward speed, step length, step height and intermediate foot lift. These parameters are calculated by a high level path planning control unit, which is beyond the scope of the current research.

The objective locomotion parameters are symbolized by:

- ν: mean horizontal hip velocity
- λ: step length, defined as the horizontal distance between both ankle joints during a double support phase
- δ: step height, being the vertical distance between both ankle joints during a double support phase
- κ: intermediate foot lift, imposing a specific vertical position of the swing foot at a given time instance during a single support phase

A robot step generally contains a single support phase and a double support phase. The single support phase is assumed to cover 80% of a total step duration, while the double support phase lasts for the remaining 20%. This corresponds to low-speed human walking.[17]

The horizontal hip velocity is ν and the total horizontal hip displacement equals the step length λ. Taking into account the 20–80% time distribution, the phase durations can then be calculated with:

$$T_S = 4T_D = \frac{4\lambda}{5\nu} \tag{3}$$

The trajectory generator establishes fifth order polynomial functions for the link angles of the supporting leg. These polynomials connect the boundary values at the start and the end of the single support phase for the position, the velocity and the acceleration of the supporting leg. Analogously, two sixth order polynomial functions for the leg links of the swing leg are established, while taking the intermediate value for the swing foot motion into account. The intermediate condition is used to lift the foot at a certain height κ, whenever an obstacle has to be avoided during the swing phase. The upper body is held in a fix position and the feet are kept horizontally during the whole trajectory.

The boundary conditions are kinematically calculated out of the start and end position of the feet given by the objective locomotion parameters; a set start point of the hip and the consideration that the hip moves with constant velocity ν at constant height.

A short double support phase is used to ensure the necessary start conditions for the next single support phase. Since both feet are in contact with the ground, a closed kinematic chain is formed by the two legs and the ground. Thus two holonomic constraints are imposed and the robot's number of degrees of freedom (DOF) is equal to three:

$$l\cos(\theta_1) + l\cos(\theta_2) - l\cos(\theta_4) - l\cos(\theta_5) = \lambda_{real} \tag{4}$$

$$l\sin(\theta_1) + l\sin(\theta_2) - l\sin(\theta_4) - l\sin(\theta_5) = \delta_{real} \tag{5}$$

with l the length of each leg link and θ_i the absolute angle of joint i measured with respect to the horizontal axis as in figure 5.

Fifth order polynomial functions are established for one leg and the upper body angle connecting the instant the swing foot touches the ground and the next single support phase. The trajectory generator establishes fifth order polynomial functions for the other leg while respecting the constraints.

In the future the method developed by Vermeulen[18] will be used to achieve faster walking. Here the trajectory planner generates motion patterns based on two specific concepts, being the use of objective locomotion parameters, and exploiting the natural upper body dynamics by manipulating the angular momentum equation. Thus taking the motion of the upper body into account and not keeping it at a fixed

https://doi.org/10.1017/S0263574705002316 Published online by Cambridge University Press

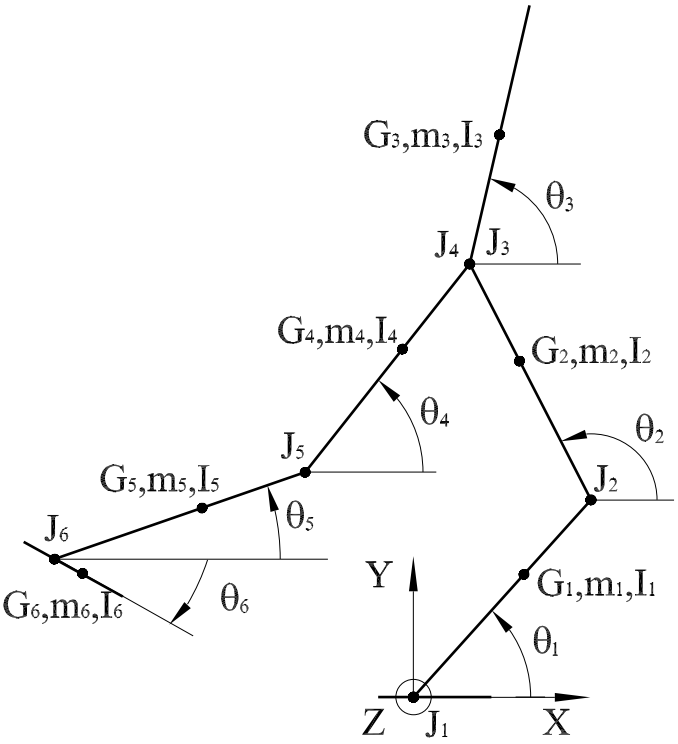

Fig. 5. Model of the biped in single support with swing foot.

angle as is the case in this paper. The effectiveness of this method has been proven in simulation.[19]

III.2. Joint trajectory tracking controller

This paragraph discusses the joint trajectory tracking controller, detailed visual information of the separate units of the tracking controller are depicted in figure 4.

III.2.1. Torque calculation. The torques required to track the reference joint trajectories are calculated based on a dynamic model of the biped robot. This dynamic model is different for single and double support phase. Thus the calculations demand a different approach for these two phases. In the next two sections the two methods are explained.

a. Computed torque during single support phase

As was mentioned before, the swing foot is kept horizontally during the leg swing. Since this foot has to be controlled, the dynamics of this link are taken into account here. The following 6 Lagrange coordinates are used to develop the computed torque controllers.

$$\mathbf{q} = [\theta_1\, \theta_2\, \theta_3\, \theta_4\, \theta_5\, \theta_6]^T \tag{6}$$

The definitions of these absolute angles are given in figure 5. During the single support phase the robot's supporting foot is assumed to remain fixed to the ground and the robot can be seen as a multi-link serial robot for which standard non-linear tracking techniques of manipulator control can be utilized. Here a computed torque method, as described in the work of Slotine,[20] is used. This method, also called feedback linearization, linearizes the non-linear input-output relation of the dynamic equations, describing the robot motion. This is a popular technique used to control mechanical systems, as was e.g. also used for the biped Johnnie.[21] The dynamic equations of the robot are written as:[22]

$$D(\mathbf{q})\ddot{\mathbf{q}} + C(\mathbf{q}, \dot{\mathbf{q}})\dot{\mathbf{q}} + G(\mathbf{q}) = \boldsymbol{\tau} \tag{7}$$

with $D(\mathbf{q})$ the inertia matrix, $C(\mathbf{q}, \dot{\mathbf{q}})$ the centrifugal/coriolis matrix, $G(\mathbf{q})$ the gravitational torque/force vector and $\boldsymbol{\tau}$ the applied torque vector.

The computed torque method determines the torque vector $\tilde{\boldsymbol{\tau}}$, which represent the net torques applied on each link. The calculation of these torques is performed by feeding forward the desired trajectory accelerations $\ddot{\tilde{\mathbf{q}}}$ and by feeding back measured positions $\mathbf{q}$ and velocities $\dot{\mathbf{q}}$ in order to cancel the non-linear centrifugal and gravitational terms. A secondary PID-feedback loop is added to influence control performance. This results in the following calculation:

$$\tilde{\boldsymbol{\tau}} = C_e(\mathbf{q}, \dot{\mathbf{q}})\dot{\mathbf{q}} + G_e(\mathbf{q}) + D_e(\mathbf{q}) \times \left[\ddot{\tilde{\mathbf{q}}} - K_p(\mathbf{q} - \tilde{\mathbf{q}}) - K_i \sum(\mathbf{q} - \tilde{\mathbf{q}}) - K_d(\dot{\mathbf{q}} - \dot{\tilde{\mathbf{q}}})\right] \tag{8}$$

The matrices D_e, C_e and G_e contain the estimated values of the inertia, centrifugal and gravitational parameters. The feedback diagonal gain matrices K_p, K_i and K_d are manually tuned.

b. Computed torque during double support phase

Immediately after impact of the swing leg, three kinematical constraints are imposed on the motion of the system. Two of them have already been introduced for the closed kinematic chain of the leg links by equations 4 and 5. The third constraint expresses that the swing foot stays on the ground, with θ_6 being constant. This constant equals zero for level ground walking. The three constraints are summarized as follows:

$$\begin{cases} \mathrm{lcos}(\theta_1) + \mathrm{lcos}(\theta_2) - \mathrm{lcos}(\theta_4) - \mathrm{lcos}(\theta_5) - \lambda_{real} = 0 \\ \mathrm{lsin}(\theta_1) + \mathrm{lsin}(\theta_2) - \mathrm{lsin}(\theta_4) - \mathrm{lsin}(\theta_5) - \delta_{real} = 0 \\ \theta_6 = constant \end{cases} \tag{9}$$

Due to these three constraint equations, the DOF during double support are reduced to 3, but the same 6 Lagrange coordinates (6) are used. The equations of motion of single support are adapted with the three geometrical constraints as follows:[23]

$$D(\mathbf{q})\ddot{\mathbf{q}} + C(\mathbf{q}, \dot{\mathbf{q}})\dot{\mathbf{q}} + G(\mathbf{q}) = \boldsymbol{\tau} + J^T(\mathbf{q})\boldsymbol{\Lambda} \tag{10}$$

With $J(\mathbf{q})$ the jacobian matrix:

$$J(\mathbf{q}) = \begin{bmatrix} -\mathrm{lsin}(\theta_1) & -\mathrm{lsin}(\theta_2) & 0 & \mathrm{lsin}(\theta_4) & \mathrm{lsin}(\theta_5) & 0 \\ \mathrm{lcos}(\theta_1) & \mathrm{lcos}(\theta_2) & 0 & -\mathrm{lcos}(\theta_4) & -\mathrm{lcos}(\theta_5) & 0 \\ 0 & 0 & 0 & 0 & 0 & 1 \end{bmatrix} \tag{11}$$

https://doi.org/10.1017/S0263574705002316 Published online by Cambridge University Press

and $\mathbf{\Lambda}$ the vector of Lagrange multipliers:

$$\Lambda = [\lambda_1\, \lambda_2\, \lambda_3]^T \tag{12}$$

Since each joint is actuated, the number of joint torques to be applied is 6. The number of DOF during double support is however reduced to 3, which makes the system over-actuated during this phase. An infinite combination of actuation torques can be applied to realize the desired trajectory tracking.

In [19] a method is described to select a specific solution based on an extended version of the method proposed by Shih and Gruver.[24] The trajectory generator of Vermeulen[18] is implemented in this paper. During single support, the polynomial reference trajectories for the leg joint angles are planned in such a way that the upper body motion is steered naturally. As a consequence, practically no ankle torque is required on the supporting leg. Only small ankle torques must be provided to compensate for modelling and approximation errors. This causes the ZMP to remain in the vicinity of the ankle joint and thus sufficiently far away from the supporting foot edges, resulting in a dynamically stable walking motion. It is therefore desirable to have the same condition of small ankle torque during double support. Moreover, small ankle torques allow these joints to be used by the ZMP observer. This module can adapt the ZMP trajectory by applying extra ankle torques in order to influence the ground reaction forces. But this issue is beyond the scope of this paper.

The joint trajectory generator used in this paper is not the full method developed by Vermeulen (III.1). Consequently, this method causes discontinuities in desired torque when transitions between single and double support occur. An alternative way to distribute torques over the actuators, is to make a linear transition of torques between the old and new single support phase, by calculating the applied torque as if the robot is in single support phase. The applied torque can be rewritten into the following form:

$$\tilde{\boldsymbol{\tau}} = (1-s)\Big(C_e(\mathbf{q},\dot{\mathbf{q}})\dot{\mathbf{q}} + G_e(\mathbf{q}) + D_e(\mathbf{q}) \times\Big[\ddot{\tilde{\mathbf{q}}} - K_p(\mathbf{q}-\tilde{\mathbf{q}}) - K_i\sum(\mathbf{q}-\tilde{\mathbf{q}}) - K_d(\dot{\mathbf{q}}-\dot{\tilde{\mathbf{q}}})\Big]\Big) \tag{13}$$

$$+ s\Big(C'_e(\mathbf{q},\dot{\mathbf{q}})\dot{\mathbf{q}} + G'_e(\mathbf{q}) + D'_e(\mathbf{q}) \times\Big[\ddot{\tilde{\mathbf{q}}} - K'_p(\mathbf{q}-\tilde{\mathbf{q}}) - K'_i\sum(\mathbf{q}-\tilde{\mathbf{q}}) - K'_d(\dot{\mathbf{q}}-\dot{\tilde{\mathbf{q}}})\Big]\Big) \tag{14}$$

with s going from $s = 0$ at impact phase until $s = 1$ at calculated lift off phase. C_e, G_e, ... are calculated as if the robot is in single support phase with the rear foot on the ground, C'_e, G'_e, ... are calculated as if the robot is in single support phase with the front foot on the ground.

The advantage of this strategy is that there are no torque discontinuities when switching between single and double support phase. The disadvantage is that the calculated torques are not dynamical correct values, but the double support phase is rather short and a feedback loop is implemented. Experimental results show this is a good strategy not causing serious problems for the regarded motions.

III.2.2. Delta-p unit. For each joint a computed torque ($\tilde{\tau}$) is available. The computed torque is then feeded into the delta-p control unit, one for each joint, which calculates the required pressure values to be set in the muscles. These two gauge pressures are generated from a mean pressure value p_m while adding and subtracting a Δp value:

$$\tilde{p_1} = p_m + \Delta p \tag{15}$$

$$\tilde{p_2} = p_m - \Delta p \tag{16}$$

Feeding back the local joint angle β and using expression (2), Δp can be determined by:

$$\Delta p = \frac{\tilde{\tau} + p_m\,[(t_2(\beta) - t_1(\beta)]}{t_2(\beta) + t_1(\beta)} \tag{17}$$

The delta-p unit is actually a feed-forward calculation from torque level to pressure level using the kinematic model of the muscle actuation system. The calculated Δp affects the torque needed to follow the desired trajectory while the mean value p_m determines the joint stiffness and can be used to influence the natural dynamics of the system. In this paper the value of p_m for each joint is set constant. A more elaborate discussion on the topic of changing stiffness and natural dynamics can be found in the publication by Verrelst et al.[12]

III.2.3. Bang-bang pressure controller. The weight of the valves controlling the muscles should be taken as low as possible. But since most pneumatic systems are designed for fixed automation purposes where weight is not an issue at all, most off-the-shelf proportional valves are far too heavy for this application. Thus a proper design of the pressure control is of great importance. In order to realize a lightweight rapid and accurate pressure control, fast switching on-off valves are used. The pneumatic solenoid valve 821 2/2 NC made by Matrix weighs only 25 g. With their reported opening times of about 1 ms and flow rate of 180 Std.l/min, they are about the fastest switching valves of that flow rate currently available.

To pressurize and depressurize the muscles, which have a varying volume up to 400 ml, a number of these small on-off valves are placed in parallel. Obviously the more valves used the higher the electric power consumption, the price and also the weight will be. Simulations of the pressure control of a constant volume resulted in a choice of two inlet and four outlet valves. The different number between inlet and outlet comes from the asymmetric pressure conditions between inlet and outlet, combined with the aim to create equal muscle's inflation and deflation times.

To connect the 6 valves into one compact pressure regulating valve two special collectors were designed. These collectors replace the original aluminium connector plates of the valves, resulting in a weight of the complete pressure regulating valve of about 150 gr. In figure 6 a section of this pressure control block is shown. Figure 7 shows a detailed view of the pressure valves with the speed-up circuit. The speed-up circuit reduces opening and closing times of the

https://doi.org/10.1017/S0263574705002316 Published online by Cambridge University Press

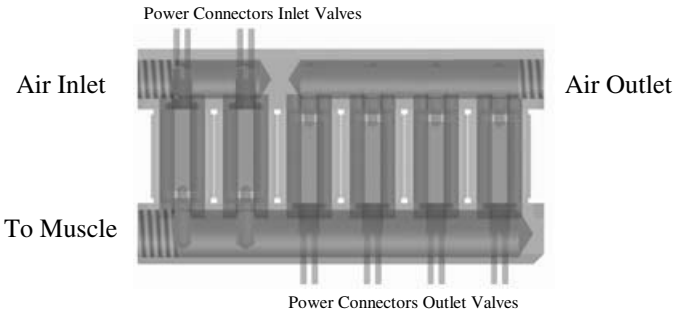

Fig. 6. Pressure control block with 2 inlet and 4 outlet valve.

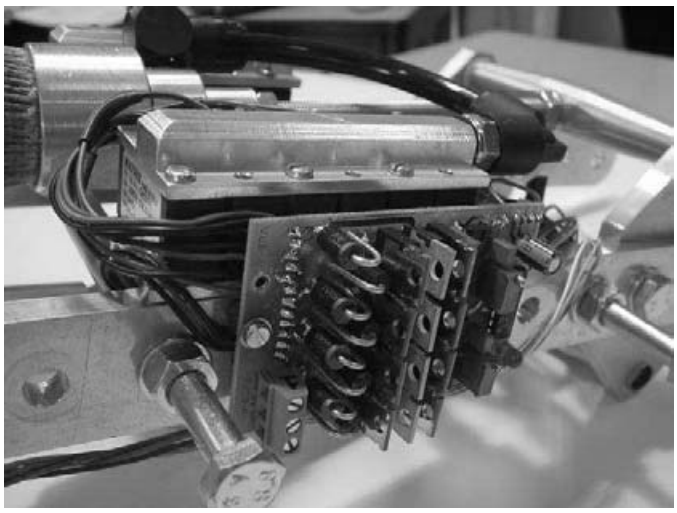

Fig. 7. Detailed view of the valves with speed up circuitry.

valves. The pressure control in a volume is achieved with a bang-bang controller with various reaction levels depending on the difference between measured and desired pressure. If this difference is large, two inlet or four outlet valves, depending on the sign of the error, are opened. If this difference is small, only one valve is switched and when the error is within reasonable limits no action will be taken, leaving the muscle closed. The principle of this control scheme is depicted in figure 8. More detailed information on the valve system can be found in the work of Van Ham et al.[25].

IV. EXPERIMENTAL RESULTS

In this section the measurements of the walking biped are shown with the following chosen objective locomotion parameters:

- mean forward velocity: $\nu = 0.02\,\text{m/s}$.
- steplength: $\lambda = 0.10\,\text{m}$
- stepheight: $\delta = 0.0\,\text{m}$
- footlift: $\kappa = 0.04\,\text{m}$

The calculated single support and double support phase durations are, respectively, 4 s and 1 s.

The graphs (10–16) depict 6 single support phases and 6 double support phases. Consequently, only data for the left leg will be shown, since this leg takes each essential configuration of the walking pattern. The graphs starts in the single support phase with the left leg as the supporting leg. Next, after a double support phase, this leg becomes the swing leg and is shifted to the front during a single support phase. Successively, another double and single support phase on the left leg brings the right leg back to the front and so on. The total shown time is approximately 30.0 s.

Due to tracking errors, the different phase transitions will not occur exactly at the calculated instants. This means that, while tracking the desired trajectories, the double and single support phases are not terminated as expected. For this reason, intermediate conditions for the trajectory generator are foreseen in the control structure. The transitions between single support and double support are detected with contact switches placed in the foot. If a double support phase ends too early, the trajectories calculated for this phase are still send to the tracking controller of the next single support phase, before calculating new trajectories. On the contrary, when a double support phase takes too long, the trajectories for the following single support phase are imposed on the system. The nature of these trajectories force the rear foot to be lifted of the ground and thus end the double support phase. Whenever the front does not touch the ground in time, the polynomial trajectories for single support phase are extended until touch-down occurs.

Figures 10, 11 and 12 show the desired and real joint angle β_i of the ankle ($i = 1$), knee ($i = 2$) and the hip ($i = 3$) respectively. The definitions of the oriented relative joint angles are giving in fig. 9 (counterclockwise positive). Vertical lines on all graphs show the phase transition instants. Due to the nature of the bang-bang pneumatic drive units and the imperfections introduced in the control loops, tracking errors can be observed. Especially when phase transitions occur, since these introduce severe changes for the control signals. But tracking errors are not that stringent as it is for e.g. welding robots, the most important thing is that the overall dynamic robot stability is guaranteed. Figure 13 visualizes the actual applied torque for the knee of the left leg, which consists of a PID feedback part and computed torque part. The computed torque controller is working well, but the robot parameters still have to be fine-tuned to lower the action of the PID controller. The pneumatics are characterized by pressure courses in both muscles of each joint. Figures 14 and

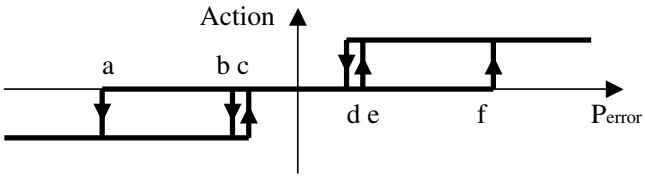

Actions

a)	*-60 mbar*	*Open all outlet valves*
b)	*-20 mbar*	*Open only one outlet valve*
c)	*-15 mbar*	*Close all outlet valves*
d)	*15 mbar*	*Close all inlet valves*
e)	*20 mbar*	*Open only one inlet valve*
f)	*60 mbar*	*Open both inlet valves*

Fig. 8. Multi-level bang-bang control scheme.

https://doi.org/10.1017/S0263574705002316 Published online by Cambridge University Press

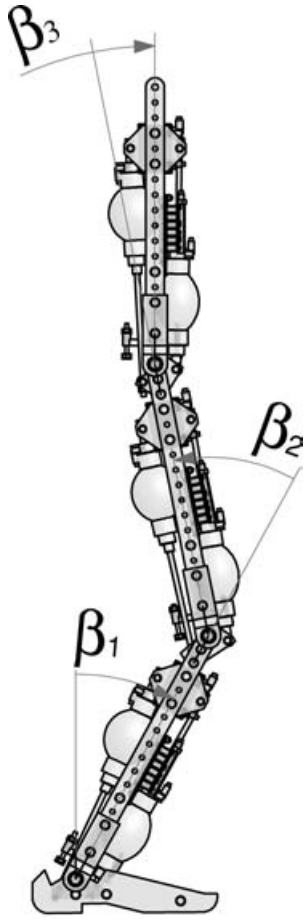

Fig. 9. Definition of the oriented relative joint angles (counter-clockwise positive).

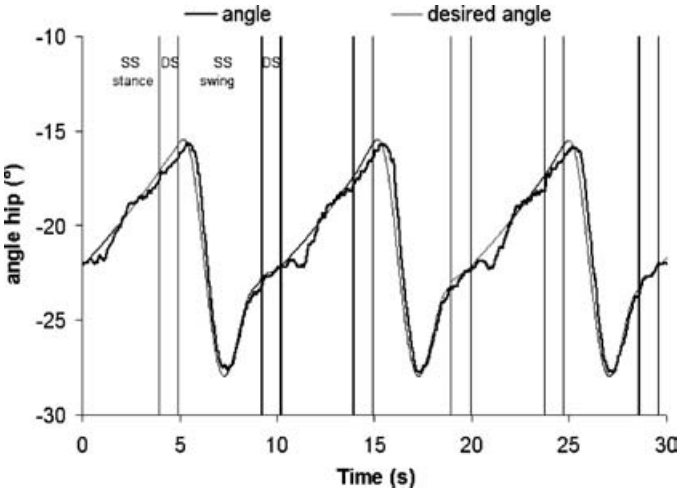

Fig. 10. Desired and measured angle of left hip joint.

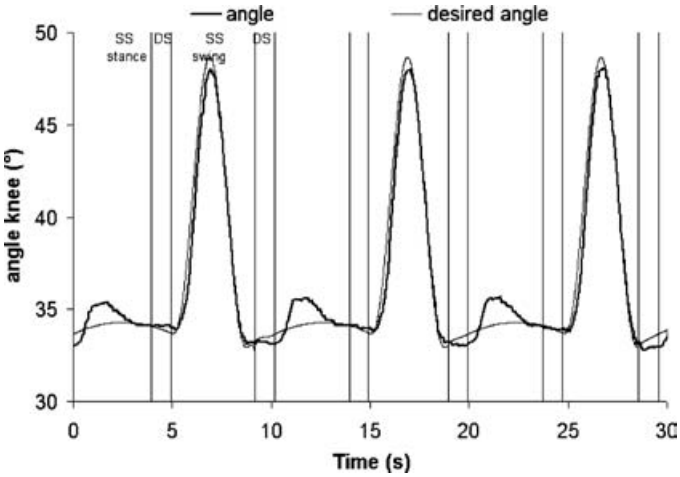

Fig. 11. Desired and measured angle of left knee joint.

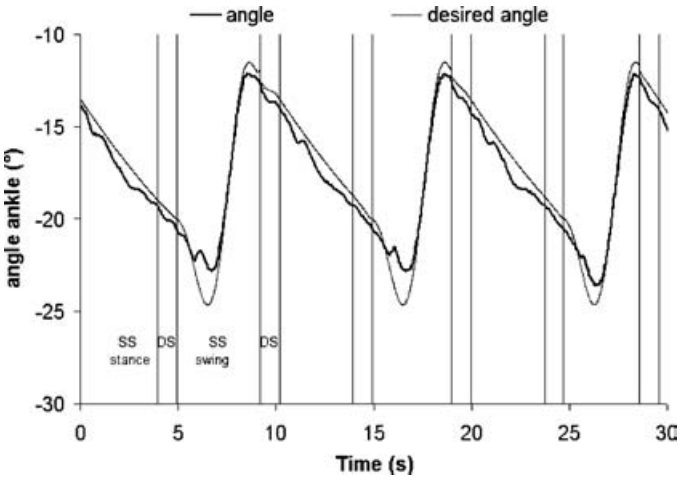

Fig. 12. Desired and measured angle of left ankle joint.

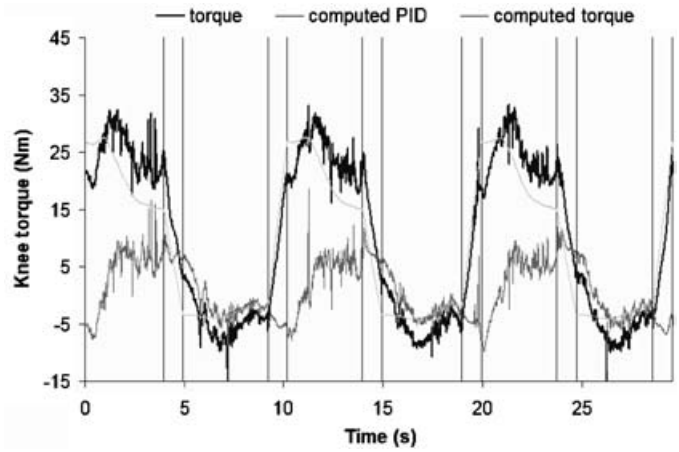

Fig. 13. Left knee torque.

15 depict desired and measured gauge pressure for the front and rear muscle of the knee of the left leg. All these graphs additionally show the valve actions taken by the respective bang-bang pressure controller. Note that in these figures a muscle with closed valves is represented by a horizontal line depicted at the 2 bar pressure level, while a small peak upwards represents one opened inlet valves, a small peak downwards one opened exhaust valves and the larger peaks represent two opened inlet or four opened outlet valves. The desired pressures are calculated by the delta-p unit. For this experiment the mean pressure p_m for all joints is taken at 2 bar, consequently the sum of the pressures in each pair of graphs, drawing the front and rear muscle pressures, is always 4 bar. It is observed that the bang-bang pressure controller is very adequate in tracking the desired pressure. Currently a lot of valve switching is required due to the fix compliance

https://doi.org/10.1017/S0263574705002316 Published online by Cambridge University Press

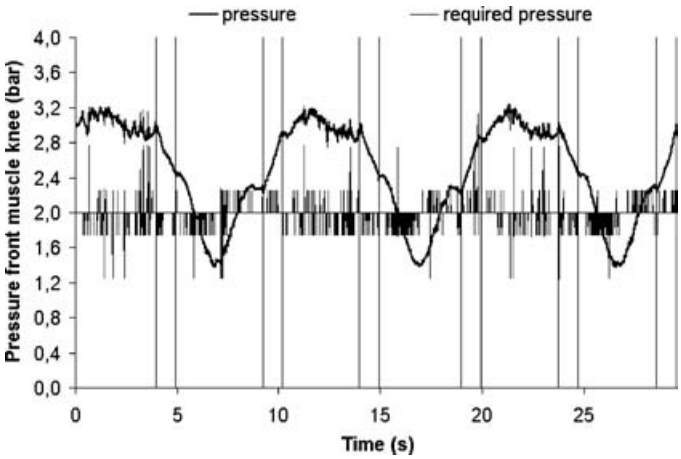

Fig. 14. Pressure and valve action of front left knee muscle.

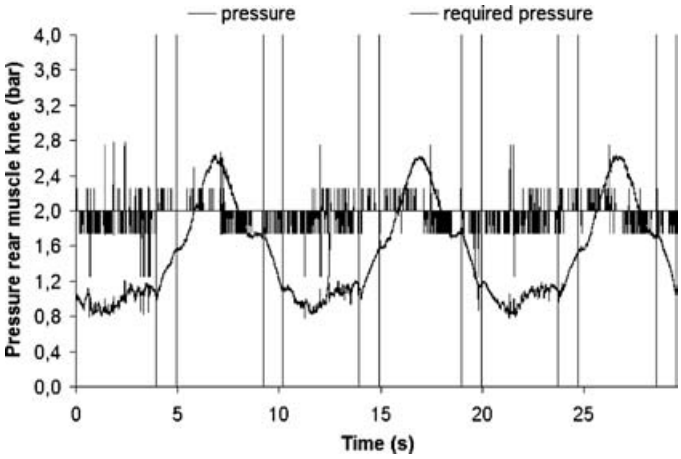

Fig. 15. Pressure and valve action of back left knee muscle.

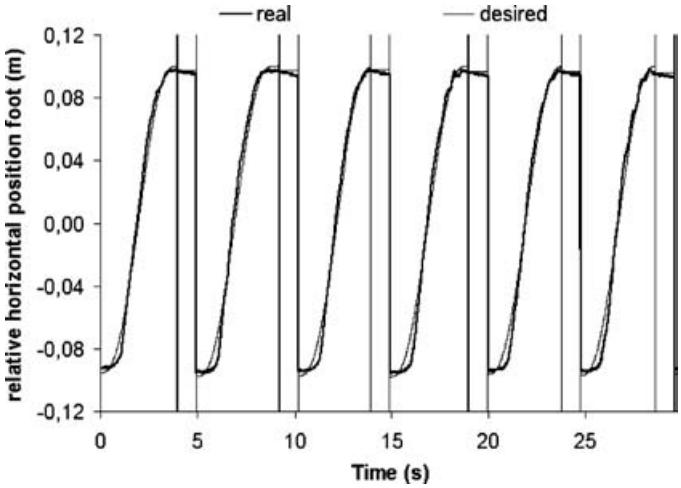

Fig. 16. Desired and real horizontal position swing foot.

setting. By incorporating the natural dynamics of the system the switching will be reduced.[12]

Figures 16 depict the horizontal position of the swing foot. Note that the swing foot moves twice the step length during single support phase. Compared with the desired objective locomotion parameter only small deviations can be observed. This proofs the global performance of the proposed control strategy. The position of the zero moment point is not measured yet and it is impossible to calculate the position out of the movements of the robot because the accelerations are not measured. In the future ground force sensors will be installed to track the ZMP. If necessary this information will be placed in an extra feedback loop to achieve postural stability during faster walking.

V. CONCLUSIONS

This paper discusses in detail the control architecture of the biped Lucy which is actuated with pleated pneumatic artificial muscles. Although not widely used in the community of legged robotics, these devices give an interesting alternative for electrical drives. They have a high power to weight ratio, can be directly coupled to actuate a joint and their inherent compliance absorb impact shocks. The adaptation of the compliance can be exploited to influence the natural dynamics of the robot in order to reduce energy consumption and control efforts which will be implemented in the near future.

The current control architecture focusses on the trajectory generator and the joint trajectory tracking controller which is divided into a computed torque controller, a delta-p unit and a pressure bang-bang controller. The formulation of the computed torque controller, given for the single support phase as well as for the double support phase, calculates the necessary joint torques needed to track the desired angular positions. The latter are generated in real-time by the trajectory generator which is based on the use of objective locomotion parameters.

The effectiveness of the proposed controller is shown by performing walking experiments. The nature of the pneumatic pressure control unit are discussed and its implications on tracking precision. Tracking errors are bounded within a maximum of a few degrees, which is a good achievement for a pneumatic system in a dynamic tracking application. The attained objective locomotion parameters show only small deviations with the desired parameters. But the most important thing is that the overall dynamic robot stability is guaranteed.

A full dynamic walking motion cannot be achieved yet since a treadmill, required to perform continuous walking experiments, is still under construction and ground reaction force sensors, to track the ZMP, still have to be installed.

Some videos of these movements can be seen at the website: http://lucy.vub.ac.be.

Acknowledgement

The author Bram Vanderborght is PhD student with a grant from the Fund for Scientific Research-Flanders (Belgium)(FWO). Lucy has been built with the financial support of the Research Council (OZR) of the Vrije Universiteit Brussel.

References

1. K. Matsuoka, "A mechanical model of repetitive hopping movements," *Biomechanics* **5**, 251–258 (1980).
2. M. Raibert, *Legged Robots That Balance* (Cambridge, Massachussetts: MIT Press, 1986).

https://doi.org/10.1017/S0263574705002316 Published online by Cambridge University Press

3. G. A. Pratt and M. M. Williamson, "Series elastic actuators," *Proceedings IEEE-IROS Conference*, Pittsburg, USA (1995) pp. 399–406.
4. J. E. Pratt and G. Pratt, "Exploiting natural dynamics in the control of a planar bipedal walking robot," *Proceedings of the 36th Annual Allerton Conference on Communication, Control, and Computing*, Monticello, Illinois (1998) pp. 739–748.
5. J. Yamgushi, D. Nishino and A. Takanishi, "Realization of dynamic biped walking varying joint stiffness using antagonistic driven joints," *Proceedings of the IEEE International Conference on Robotics and Automatisation*, Leuven, Belgium (1998) pp. 2022–2029.
6. J. W. Hurst, J. Chestnutt and A. Rizzi, "An actuator with physically variable stiffness for highly dynamic legged locomotion," *Proceedings of the 2004 International Conference on Robotics and Automation* (May, 2004) pp. 4662–4667.
7. F. Daerden and D. Lefeber, "The concept and design of pleated pneumatic artificial muscles," *International Journal of Fluid Power* **2**, No. 3, 41–50 (2001).
8. R. Q. van der Linde, "Active leg compliance for passive walking," *Proceedings of the IEEE International Conference on Robotics and Automatisation*, Leuven, Belgium (1998) pp. 2339–2344.
9. M. Wisse and F. van Frankenhuyzen, "Design and construction of mike: A 2d autonomous biped based on passive dynamic walking," *Proceedings of the Conference on Adaptive Motion of Animals and Machines*, Kyoto, Japan (2003) CD.
10. S. T. Davis and D. G. Caldwell, "The bio-mimetic design of a robot primate using pneumatic artificial muscle actuators," *Proceedings of the 4th International Conference on Climbing and Walking Robots, from Biology to Industrial Application*, Karlsruhe, Germany (2001) pp. 197–204.
11. http://www.shadow.org.uk
12. B. Verrelst, R. V. Ham, B. Vanderborght, J. Vermeulen, D. Lefeber and F. Daerden, "Exploiting adaptable passive behaviour to influence natural dynamics applied to legged robots," *Robotica* **23**, Part 2, 149–158 (2005).
13. H. F. Schulte, "The characteristics of the McKibben artificial muscle," *The Application of External Power in Prosthetics and Orthotics* (Lake Arrowhead: National Academy of Sciences–National Research Council, 1961) No. 874, pp. 94–115.
14. F. Daerden, "Conception and Realization of Pleated Pneumatic Artificial Muscles and their Use as Compliant Actuation Elements," *PhD thesis* (Vrije Universiteit Brussel, 1999).
15. C. E. Bauby and A. D. Kuo, "Active control of lateral balance in human walking," *Journal of Biomechanics* **33**, 1433–1440 (2000).
16. B. Verrelst, R. V. Ham, B. Vanderborght, F. Daerden and D. Lefeber, "The pneumatic biped "lucy" actuated with pleated pneumatic artificial muscles," *Autonomous Robots* **18**, 201–213 (2005).
17. M. Hardt, K. Kruetz-Delgado, J. Helton and O. V. Stryck, "Obtaining minimum energy biped walking gaits with symbolic models and numerical optimal control," *Proceedings of the Workshop- Biomechanics Meets Robotics, Modelling and Simulation of Motion*, Heidelberg, Germany (1999) pp. 1–19.
18. J. Vermeulen, B. Verrelst, D. Lefeber, P. Kool and B. Vanderborght, "A real-time joint trajectory planner for dynamic walking bipeds in the sagittal plane," *Robotica* (in press).
19. B. Verrelst, J. Vermeulen, B. Vanderborght, R. Van Ham, J. Naudet, D. Lefeber, F. Daerden and M. Van Damme, "Motion generation and control for the pneumatic biped lucy," *International Journal of Humanoid Robotics* (in press).
20. J. J. E. Slotine and W. Li, *Applied Nonlinear Control* (Cambridge, MA.: Prentice-Hall, 1991).
21. K. Löffler, M. Gienger and F. Pfeiffer, "Simulation and control of a biped jogging robot," *Proceedings on the 4th International Conference on Climbing and Walking Robots: From Biology to Industrial Applications CLAWAR 2001* (K. Berns and R. Dillmann, eds.) (Professional Engineering Publishing, 2001) pp. 867–874.
22. M. Spong and M. Vidyasagar, *Robot Dynamics and Control* (JohnWiley and Sons, 1989).
23. J. G. Jalón and E. Bayo, *Kinematic and Dynamic Simulation of Multibody Systems – The Real-Time Challange* (Springer-Verlag, 1994).
24. C.-L. Shih and W. Gruver, "Control of a biped robot in the double-support phase," *IEEE Transactions on Systems, Man and Cybernetics* **22**, No. 4, 729–735 (1992).
25. R. Van Ham, B. Verrelst, F. Daerden, B. Vanderborght and D. Lefeber, "Fast and accurate pressure control using on-off valves," *International Journal of Fluid Power* **6**, 53–58 (March, 2005).

https://doi.org/10.1017/S0263574705002316 Published online by Cambridge University Press